Phase stability and pressure-induced semiconductor to metal transition in crystalline $GeSe_2$

2002 J. Phys.: Condens. Matter 14 9589

(http://iopscience.iop.org/0953-8984/14/41/314)

INSTITUTE OF PHYSICS PUBLISHING JOURNAL OF PHYSICS: CONDENSED MATTER

J. Phys.: Condens. Matter **14** (2002) 9589–9600 PII: S0953-8984(02)39693-0

Phase stability and pressure-induced semiconductor to metal transition in crystalline $GeSe_2$

M Fuentes-Cabrera, H Wang and Otto F Sankey

Department of Physics and Astronomy, Arizona State University, Tempe, AZ 85287-1504, USA

Received 17 July 2002
Published 4 October 2002
Online at stacks.iop.org/JPhysCM/14/9589

Abstract

The structural and electronic properties of crystalline $GeSe_2$ are studied using *ab initio* density functional theory. $GeSe_2$ exists in a variety of phases; here eight phases, six previously synthesized and two hypothetical, are investigated within the local density approximation and the generalized gradient approximation (GGA). The results show that the GGA correctly describes the energetics of the $GeSe_2$ even with variations in charge density of layer $GeSe_2$ structures. The stability of the phases studied is discussed, and the possible phase transitions under pressure are predicted and compared to experiment. The electronic structure of $GeSe_2$ confirms, for the first time, that the high-pressure CdI_2-type phase is metallic which may produce the semiconductor to metal transition in the $GeSe_2$ system under pressure.

1. Introduction

Crystalline and amorphous germanium diselenide semiconductors have many interesting properties, as well as many potential applications such as in optoelectronic and IR optical devices, optical storage and photosensitive material and solar cells. Numerous studies, utilizing both experimental and theoretical approaches, have been carried out to better understand the pressure-induced structural and electronic properties of $GeSe_2$ [1–11]. There are three stable crystalline phases of $GeSe_2$ reported in the literature. Orthorhombic α-$GeSe_2$ ($Pmmm$ or Pmn) is the low-temperature modification of $GeSe_2$, and has a distorted layered structure of CdI_2, where the cations are octahedrally coordinated [12, 13]. Layered β-$GeSe_2$ ($P2_1/c$) is isotypic with the high-temperature modification of the sulfur compound GeS_2. Here the $GeSe_4$ tetrahedra are connected via corners into chains along the a axis and by edge-sharing Ge_2Se_8 double tetrahedra along the b axis [14–18]. The third phase γ-$GeSe_2$ has a structure related to hexagonal $SnSe_2$ of the CdI_2 type [19]. The CdI_2-type structure has a hexagonal symmetry with a layer structure. The stability of different polymorphs of $GeSe_2$ has been discussed by Stølen *et al* [20]. Of course, $GeSe_2$ forms amorphous networks as well, which have been studied both experimentally [2] and theoretically [11]. $GeSe_2$ has a remarkable complexity with a variety of structural forms. This paper will focus only on the crystalline phases.

0953-8984/02/419589+12$30.00

Pressure-induced phase transitions are an attractive topic and active field. High pressure is able to produce new structures as a result of new chemistry that occurs from mild or even extreme changes in the bonding. Pressure-induced phase transitions in $GeSe_2$, especially the semiconductor–metal transition, are not well understood. Prasad *et al* [10] studied Ge_xSe_{100-x} ($0 \leqslant x \leqslant 40$) glasses up to 14 GPa and temperatures of 77–298 K. They observed a discontinuous glassy semiconductor to metallic phase transition. This shows that the electronic properties of the chalcogenide glass $GeSe_2$ can be permanently changed by applying pressure. Several high-pressure experiments have been conducted recently [4, 5] in crystalline $GeSe_2$ to unravel the mechanism of this transition. It was found that $GeSe_2$ crystallizes in the CdI_2-type phase at around 7 GPa and it was suggested that this phase is metallic. The mechanism of the pressure-induced semiconductor to metal transition was then explained by a structural phase transition to a CdI_2-like phase.

In this study, we investigate the structural and electronic properties of eight phases of $GeSe_2$ with *ab initio* density functional techniques [21, 22]. The *ab initio* method is based on pseudo-potential–density functional theory within the local density approximation (LDA) and the generalized gradient approximation (GGA). A plane-wave basis set is used and convergence is enhanced using ultrasoft pseudo-potentials [22, 23]. The integrations over the Brillouin zone were carried out by the Monkhorst–Pack scheme [24]. For the LDA we use the Ceperly–Alder expression [25, 26] while the Perdew–Wang expression [27] was used for the GGA.

In section 2 of this paper, we describe the structural properties of the phases studied and discuss the optimized structures from geometry optimization using the LDA and GGA. We find that the LDA results for the structural parameters are in good agreement with experiments, where the GGA results are in moderate agreement. In section 3, we investigate the energetics and phase transition properties, and predict a sequence of phase transitions for the $GeSe_2$ system. Here we find that the GGA gives the best agreement with experiments. The electronic properties are studied in section 4 and our electronic structures of $GeSe_2$ confirm that the CdI_2-type phase is metallic. Finally we conclude in section 5.

2. Structural properties and relaxation results

$GeSe_2$ has a remarkable variety of crystalline structures. We will systematically study several of these structures theoretically to determine their electronic properties, energetics, equations of state and possible high-pressure phase transitions. Table 1 contains a list, and a brief description, of several existing or potential phases of crystalline germanium selenide. All of them, except Ge_4Se_9, are studied in this work. The theoretical investigation of the structural and electronic properties of Ge_4Se_9 will be reported in future work, and is listed here only for completeness.

Among the phases studied in this work, six have been examined experimentally and two are hypothetical porous phases. The two hypothetical porous phases are being investigated for comparative purposes, and to assess the likelihood of future synthesis. We now give a brief description of the eight studied phases. Figures 1(a)–(h) show their crystalline structure.

$GeSe_2$ crystallizes in the monoclinic structure β-$GeSe_2$ ($P2_1/c$), and is experimentally the most stable [17] among the phases of $GeSe_2$ listed in table 1. Figure 1(a) shows its structure, and the fundamental building block consists of a $GeSe_4$ tetrahedron which is shown by figure 1(i). β-$GeSe_2$ ($P2_1/c$) is a two-dimensional structure with layers made up of $GeSe_4$ tetrahedra. Within each layer, one half of the $GeSe_4$ tetrahedra are linked at the corners through the Se atoms, and the other half are linked by their edges. The next structure is HgI_2 ($P4_2/nmc$) which is shown in figure 1(b). It is an intermediate phase between β-$GeSe_2$ ($P2_1/c$) and cristobalite-like $I\bar{4}2d$ structures [30]. Layers made up of $GeSe_4$ tetrahedra are linked by

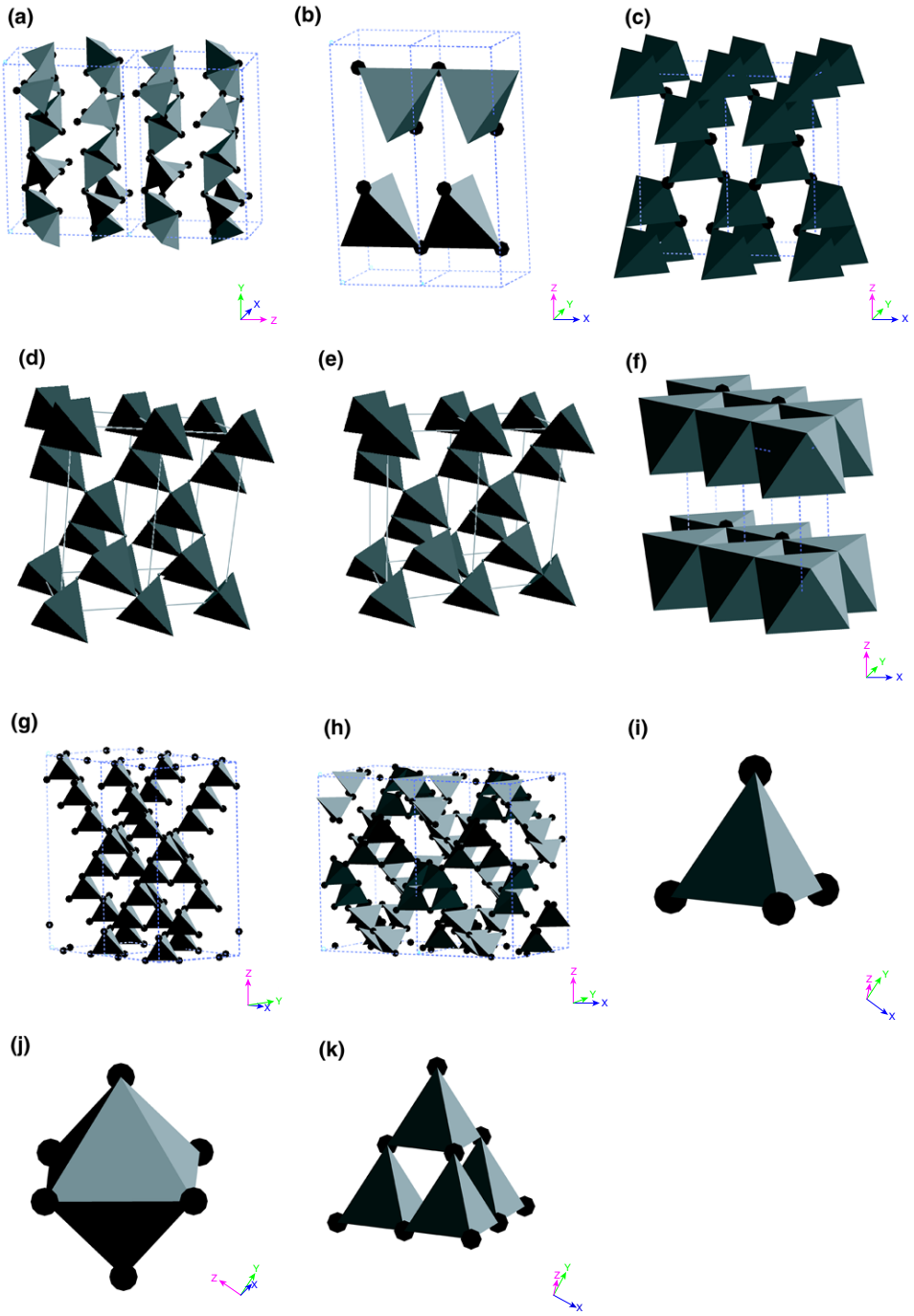

Figure 1. (a)–(h) Structures of the $GeSe_2$ studied. (i)–(k) The building blocks of the structures studied. (a) β; (b) HgI_2 type; (c) T_1-cristobalite; (d) $I\bar{4}$; (e) $P\bar{4}$; (f) CdI_2 type; (g) T_2-cristobalite; (h) δ and (i) tetrahedron $T_1 = GeSe_4$; (j) octahedron $GeSe_6$; (k) supertetrahedron $T_2 = Ge_4Se_{10}$.
(This figure is in colour only in the electronic version)

Table 1. Phases and descriptions of germanium selenide studied. A dagger (†) indicates a hypothetical phase.

Phase	Space group	Properties
β-phase [17]	$P2_1/c$	2D material with layers made up of $T_1 = GeSe_4$ tetrahedral units; 50% of $GeSe_4$ are connected by the corners and 50% by the edges.
HgI_2 type [28]	$P4_2/nmc$	2D material with layers made up of T_1 units. All of T_1 are connected by the corners.
T_1-cristobalite [5, 29]	$I\bar{4}2d$	3D material made up of T_1 units connected by the corners.
$I\bar{4}$-phase [4]	$I\bar{4}$	3D material made up of T_1 units connected by the corners.
$P\bar{4}$-phase [4]	$P\bar{4}$	3D material made up of T_1 units connected by the corners.
CdI_2 type [29]	$P\bar{3}m1$	2D material with layers made up of $GeSe_6$ octahedral units; $GeSe_6$ are connected by the corners and edges.
T_2-cristobalite†	$I\bar{4}2d$	3D hypothetical microporous material made up of $T_2 = Ge_4Se_{10}$ supertetrahedral units connected by the corners.
δ-phase†	$I4_1/acd$	3D hypothetical microporous material made up of two interpenetrating Ge_4Se_8. The T_2s are connected by the corners.
Ge_4Se_9 [3]	$Pca2_1$	2D material made up of T_1 units. All T_1s are connected by the corners.

the corners to form a two-dimensional-like structure. The structure of T_1-cristobalite (the T_1 designation is defined below) is shown in figure 1(c). It is a three-dimensional structure and is made up of $GeSe_4$ tetrahedra linked to each other by sharing the Se atoms at the corners. The arrangement of the $GeSe_4$ tetrahedra coincides with the arrangement of the SiO_4 tetrahedra in T_1 cristobalite SiO_2; hence we refer to this $GeSe_2$ structure as T_1-cristobalite. The other two three-dimensional crystalline $GeSe_2$ structures in table 1 are the high-pressure phases $I\bar{4}$ and $P\bar{4}$ observed by Grzechnik *et al* [4]. They are shown in figures 1(d) and (e), respectively. Both $I\bar{4}$ and $P\bar{4}$ variants are a slight distortion of $I\bar{4}2d$; the distortion consists of small displacements of the Se atoms in the y and z directions. In the ideal $I\bar{4}2d$ case, the y and z atomic coordinates for the symmetry-equivalent Se atoms are fixed at $1/4$ and $1/8$. Displacements, lower the symmetry of the lattice, produce a nonequivalency of the Ge and/or Se atoms. This is analogous to the SiO_2 case where either $I\bar{4}$ or $P\bar{4}$ structures are produced by distortions of the $I\bar{4}2d$ cristobalite [31, 32]. The CdI_2 ($P\bar{3}m1$) two-dimensional structure differs from other two-dimensional structures studied in this work. Its building block is the $GeSe_6$ octahedra as shown in figure 1(j). The octahedra in CdI_2 are arranged in layers linked by the edges and the corners, as seen in figure 1(f).

The investigation of hypothetical porous phases of $GeSe_2$ is motivated by the great interest in the synthesis of open framework materials with large pores. Materials with large pores such as zeolites are used in 'oil cracking', and may even act as antidot semiconductors. An antidot is a subnanometre vacancy that can trap electrons from the surrounding material [33]. Large-pore semiconductors or insulators impact the fields of nanotechnology, molecular sieve science and optoelectronics [34–38].

It has been proposed [35] that nanometre-scale pores within a new class of porous materials, know as supertetrahedral solids, can trap electrons in an antidot. A supertetrahedron is a

tetrahedron built of fundamental tetrahedra. A T_1-tetrahedron (GeS_4) is a simple fundamental tetrahedron and is shown in figure 1(i). A T_2-supertetrahedron (Ge_4S_{10}) is built of four fundamental tetrahedra (Ge_2S_4) sharing corners. The supertetrahedron itself is linked to other supertetrahedra to form a supertetrahedral solid. This technique is called decoration [40], in which a more complex solid is built by replacing simple units with more complex ones. Applying this technique here, one starts from a tetrahedral structure and theoretically replaces each tetrahedron by a supertetrahedron. For example, consider the $GeSe_2$ tetrahedral solid made up of corner-linked $GeSe_4$ tetrahedra in the cristobalite structure ($I\bar{4}2d$). It can be decorated by theoretically replacing each $GeSe_4$ by the supertetrahedron $Ge_{t_n}Se_{t_{(n+1)}}$. As a result, one obtains the supertetrahedral solid $Ge_{t_n}Se_{t_{(n+1)}-2}$, which we call T_n-cristobalite. The original starting structure is simply T_1-cristobalite. Because the size of the pores of T_n-cristobalite increases rapidly with n, the decoration technique provides a recipe for creating materials with very large pores, making this technique an important tool to guide synthesis.

$GeSe_2$ in the T_2-cristobalite structure is shown in figure 1(g). It is made up of T_2 (Ge_4Se_{10}, figure 1(k)) supertetrahedra connected through the Se atoms on the corners. The structure of δ-$GeSe_2$ illustrated by figure 1(h) is made up of two interpenetrating T_2-cristobalite frameworks, which is analogous to that of δ-GeS_2, which has been synthesized by MacLachlan *et al* [39].

Earlier theoretical work [35] found that the pores of supertetrahedral (T_3) $In_{10}S_{18}^{6-}$ contain particle-in-a-box (PIAB) 'deep-level' electron states within the bandgap. Here we investigate whether the pores of supertetrahedral $GeSe_2$ materials contain PIAB 'deep-level' electron states as well. To our knowledge, porous materials of germanium selenide have not yet been synthesized. Here the structural and electronic properties of $GeSe_2$ T_2-cristobalite and δ-$GeSe_2$, two hypothetical neutral supertetrahedral porous phases, are examined.

All the structures were relaxed using an *ab initio* density functional method [21, 22] combined with a conjugate gradient technique method to allow for variations in the shape of the cell and in the atomic positions. The eigenstates were expanded in plane waves, and the simulation is converged using an energy cutoff of 11.4 Ryd. The k-point sampling grid depended on the chosen structure. The simulation converged with ten k-points for β, 18 k-points for HgI_2 type, 20 k-points for CdI_2 type, 12 k-points for $I\bar{4}$, eight k-points for $P\bar{4}$ and 11 k-points for T_1-cristobalite, T_2-cristobalite and δ.

We have minimized the energy to give the equilibrium coordinates (in fractional coordinates) for β, CdI_2-type, HgI_2-type, T_1-cristobalite, $I\bar{4}$, $P\bar{4}$, T_2-cristobalite and δ structures. The relaxed parameters for the equilibrium systems are listed in table 2. Experimental results are included for comparison where available. We give theoretical values using both the LDA and the GGA. Inspection shows that the LDA and experimental results are in good agreement overall, while the GGA results are less satisfactory. The lattice parameters for the minimum energy structure are shown in tables 3 and 4. The experimental values for the lattice parameters of β, T_1-cristobalite, CdI_2 type, $I\bar{4}$ and $P\bar{4}$ are also in better agreement with the LDA values than for those of the GGA. In general, we find that the GGA overestimates and the LDA underestimates the lattice parameters. In the next section, we will find that although the lattice parameters using the GGA are not as accurate, the energetics are better reproduced than with the LDA.

3. Energetics and transition properties

We determine the LDA and GGA equation of state for each of our structures. This information is useful in predicting phase transitions under pressure. We fit the energy versus volume curves to a Birch–Murnaghan equation of state [41]. This fit is summarized in table 5 which includes the minimum energy E_0, equilibrium volume V_0, bulk modulus K and pressure derivative of

Table 2. Equilibrium positions (fractional coordinates) of the atoms in different phases of $GeSe_2$.

Atom	Site	LDA	GGA	Experiment [17]
β-phase				
Ge(1)	4e(x, y, z)	(0.335, 0.158, 0.230)	(0.315, 0.161, 0.223)	(0.3442, 0.1537, 0.2209)
Ge(2)	4e(x, y, z)	(0.158, 0.144, 0.780)	(0.117, 0.148, 0.771)	(0.1717, 0.1494, 0.7773)
Ge(3)	4e(x, y, z)	(0.828, 0.997, 0.709)	(0.805, 0.995, 0.717)	(0.8414, 0.0008, 0.7017)
Ge(4)	4e(x, y, z)	(0.675, 0.313, 0.286)	(0.629, 0.318, 0.277)	(0.6752, 0.3090, 0.2734)
Se(1)	4e(x, y, z)	(0.675, 0.181, 0.216)	(0.636, 0.192, 0.208)	(0.6757, 0.1770, 0.2095)
Se(2)	4e(x, y, z)	(0.268, 0.040, 0.120)	(0.267, 0.044, 0.131)	(0.2778, 0.0357, 0.1191)
Se(3)	4e(x, y, z)	(0.224, 0.118, 0.417)	(0.222, 0.121, 0.387)	(0.2305, 0.1156, 0.4002)
Se(4)	4e(x, y, z)	(0.134, 0.256, 0.135)	(0.118, 0.256, 0.142)	(0.1647, 0.2559, 0.1326)
Se(5)	4e(x, y, z)	(0.420, 0.326, 0.419)	(0.378, 0.330, 0.391)	(0.4278, 0.3302, 0.4028)
Se(6)	4e(x, y, z)	(0.912, 0.355, 0.427)	(0.877, 0.344, 0.397)	(0.9199, 0.3373, 0.4048)
Se(7)	4e(x, y, z)	(0.664, 0.396, 0.118)	(0.626, 0.406, 0.139)	(0.6751, 0.3926, 0.1145)
Se(8)	4e(x, y, z)	(0.181, 0.482, 0.186)	(0.138, 0.474, 0.192)	(0.1738, 0.4779, 0.1939)
CdI_2-type				
Ge(1)	1a(0, 0, 0)	(0, 0, 0)	(0, 0, 0)	—
Se(1)	2d($\frac{1}{3}$, $\frac{2}{3}$, z)	(0.333, 0.666, 0.261)	(0.33, 0.66, 0.225)	—
HgI_2-type				
Ge(1)	2a($\frac{3}{4}$, $\frac{1}{4}$, $\frac{3}{4}$)	(0.750, 0.250, 0.750)	(0.750, 0.250, 0.750)	—
Se(1)	2d($\frac{1}{4}$, $\frac{1}{4}$, z)	(0.250, 0.250, 0.393)	(0.250, 0.250, 0.376)	—
T_1-cristobalite				
Ge(1)	4a(0, 0, 0)	(0, 0, 0)	(0, 0, 0)	(0, 0, 0)
Se(1)	8d(x, $\frac{1}{4}$, $\frac{1}{8}$)	(0.261, 0.25, 0.125)	(0.238, 0.25, 0.125)	(0.2495, 0.25, 0.125)
$I\bar{4}$-phase				
Ge(1)	2a(0, 0, 0)	(0, 0, 0)	(0, 0, 0)	(0, 0, 0)
Ge(2)	2c(0, 0.5, 0.25)	(0, 0.5, 0.25)	(0, 0.5, 0.25)	(0, 0.5, 0.25)
Se(1)	8g(x, y, z)	(0.767, 0.249, 0.126)	(0.735, 0.250, 0.125)	(0.7622, 0.2605, 0.1282)
$P\bar{4}$-phase				
Ge(1)	1a(0, 0, 0)	(0, 0, 0)	(0, 0, 0)	(0, 0, 0)
Ge(2)	1d(0.5, 0.5, 0.5)	(0.5, 0.5, 0.5)	(0.5, 0.5, 0.5)	(0.5, 0.5, 0.5)
Ge(3)	2g(0, 0.5, 0.25)	(0, 0.5, 0.25)	(0, 0.5, 0.25)	(0, 0.5, 0.25)
Se(1)	4h(x, y, z)	(0.267, 0.249, 0.126)	(0.241, 0.249, 0.126)	(0.2739, 0.2340, 0.1280)
Se(2)	4h(x, y, z)	(0.767, 0.750, 0.625)	(0.742, 0.750, 0.625)	(0.7711, 0.7700, 0.6273)
T_2-cristobalite				
Ge(1)	16e(x, y, z)	(0.126, 0.101, −0.064)	(0.127, 0.097, −0.063)	—
Se(1)	16e(x, y, z)	(0.038, 0.249, 0.006)	(0.034, 0.245, 0.001)	—
Se(2)	8c(0, 0, z)	(0.000, 0.000, 0.143)	(0.000, 0.000, 0.138)	—
Se(3)	8d(x, $\frac{1}{4}$, $\frac{1}{8}$)	(−0.234, 0.250, 0.125)	(−0.222, 0.250, 0.125)	—
δ-phase				
Ge(1)	32g(x, y, z)	(0.373, 0.357, 0.062)	(0.375, 0.334, 0.061)	—
Se(1)	16d(0, $\frac{1}{4}$, z)	(0.000, 0.250, 0.013)	(0.000, 0.250, 0.016)	—
Se(2)	16e(x, 0, $\frac{1}{4}$)	(0.259, 0.000, 0.250)	(0.303, 0.000, 0.250)	—
Se(3)	32g(x, y, z)	(0.023, −0.005, 0.374)	(0.042, 0.022, 0.376)	—

the bulk modulus K'. The bulk modulus supplies a rough figure concerning the hardness of a material.

The Birch–Murnaghan fits of the LDA and GGA energy versus volume curves are illustrated in figures 2(a) and (b), respectively. The GGA and LDA give quite different predictions for the most stable structure of $GeSe_2$ as can be seen in figure 2. The LDA predicts

Table 3. Equilibrium lattice parameters of β-phase $GeSe_2$.

	a_0 (Å)	b_0 (Å)	c_0 (Å)	β (deg)	Volume (Å^3)
Theory LDA	6.90	16.84	11.30	91.50	1307.40
Theory GGA	7.24	17.53	13.22	91.35	1677.29
Experiment [17]	7.016	16.796	11.831	90.65	1394.00

Table 4. Equilibrium lattice parameters of seven $GeSe_2$ phases.

	a_0 (Å)	c_0 (Å)	c_0/a_0	Volume (Å^3)
CdI_2 type				
Theory LDA	3.55	5.78	1.63	63.25
Theory GGA	3.62	6.76	1.87	76.70
Experiment [29]	4.03	5.89	1.46	82.84
HgI_2 type				
Theory LDA	3.66	10.67	2.92	142.98
Theory GGA	3.73	12.17	3.26	169.43
Experiment	—	—	—	—
T_1-cristobalite				
Theory LDA	5.44	10.20	1.88	301.52
Theory GGA	5.99	9.76	1.63	350.19
Experiment [5]	5.7307	9.691	1.69	318.30
$I\bar{4}$-phase				
Theory LDA	5.53	9.88	1.79	301.79
Theory GGA	5.98	9.77	1.64	349.15
Experiment [4]	5.507	9.937	1.80	301.41
$P\bar{4}$-phase				
Theory LDA	5.49	10.00	1.82	300.98
Theory GGA	5.90	10.01	1.70	348.36
Experiment [4]	5.339	10.036	1.88	286.07
T_2-cristobalite				
Theory LDA	11.06	19.61	1.77	2396.60
Theory GGA	11.51	20.51	1.79	2717.17
Experiment	—	—	—	—
δ-phase				
Theory LDA	10.96	20.28	1.85	2436.03
Theory GGA	12.28	20.07	1.63	3026.52
Experiment	—	—	—	—

that T_1-cristobalite is the lowest-energy structure, while the GGA identifies β as the lowest-energy structure. Based on the available experiments, β is the most stable [17, 20] among all the structures studied. Therefore, the GGA appears to be correctly describing the energetics of the $GeSe_2$ system. The failure of the LDA is probably caused by the large variations in the electron density of the layered structures studied (such as β-$GeSe_2$). The stability of the two hypothetical porous phases of $GeSe_2$ can be determined by the results presented in figure 2(b) for the GGA. It is seen that the T_2-cristobalite and the δ are indeed very low-energy structures of germanium diselenide. Remarkably, the T_2-cristobalite structure is nearly twice the volume/atom of the other structures, yet is only about 10 meV/atom higher in energy than the β-phase.

Pressure-induced phase transitions in crystalline $GeSe_2$ can now be investigated. Several experiments have been reported concerning the high-pressure behaviour of crystalline and

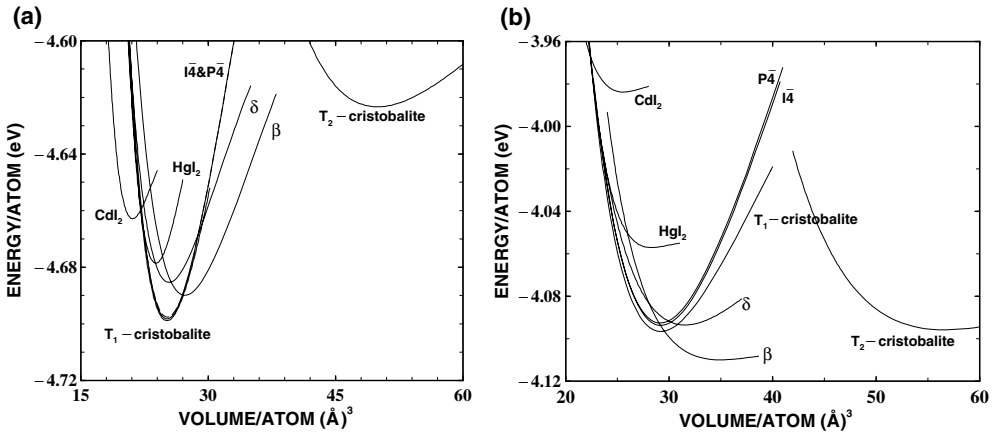

Figure 2. Equations of state for the structures studied. (a) Birch–Murnaghan fitting to the LDA energy versus volume curve. (b) Birch–Murnaghan fitting to the GGA energy versus volume curve.

Table 5. Birch–Murnaghan parameters obtained with LDA (GGA). E_0 is the minimum energy, V_0 is the equilibrium volume, K is the bulk modulus and K' is the pressure derivative of the bulk modulus.

System	E_0 (eV/atom)	V_0 (Å^3/atom)	K (GPa)	K'
β-phase	−4.69 (−4.11)	27.24 (34.94)	13.18 (2.47)	6.90 (13.73)
CdI_2 type	−4.66 (−3.98)	21.08 (25.57)	28.17 (6.95)	13.80 (6.52)
HgI_2 type	−4.68 (−4.06)	23.83 (28.24)	34.92 (7.46)	9.16 (17.98)
T_1-cristobalite	−4.70 (−4.10)	25.13 (29.18)	23.53 (13.65)	6.56 (6.40)
$I\bar{4}$-phase	−4.70 (−4.09)	25.15 (29.10)	23.37 (15.53)	6.37 (4.89)
$P\bar{4}$-phase	−4.70 (−4.09)	25.08 (29.03)	25.04 (15.50)	6.33 (4.80)
T_2-cristobalite	−4.62 (−4.10)	49.93 (56.61)	3.75 (2.66)	6.36 (9.64)
δ-phase	−4.69 (−4.09)	25.38 (31.53)	17.40 (6.30)	8.12 (6.60)

Table 6. Experimentally determined high-pressure phases of $GeSe_2$.

Phase	Pressure (GPa)	Temperature
$I\bar{4}$-phase [4]	2	698 K
T_1-cristobalite [29]	1–5	500 °C
T_1-cristobalite [5, 29]	3	500 °C
HgI_2 type [5, 6, 28]	3	400 °C
CdI_2 type [29]	5	400 °C
$P\bar{4}$-phase [4]	6	773 K

glassy $GeSe_2$. The two sequences of phase transitions, β-$GeSe_2 \rightarrow HgI_2 \rightarrow$ cristobalite and β-$GeSe_2 \rightarrow HgI_2 \rightarrow CdI_2$, can be inferred from the high-pressure, high-temperature phase diagram of HT-GeS_2 [28], isostructural with β-$GeSe_2$ [6]. Table 6 summarizes the available experimental results of the temperature and pressure under which β transforms to $I\bar{4}$, T_1-cristobalite, HgI_2 type, CdI_2 type and $P\bar{4}$. The results concerning the HgI_2-type $GeSe_2$ are ambiguous in the literature; Grzechnik *et al* [6] noted that the combined results of Shimizu and Kobayashi [28] and Grande *et al* [5] confirm that β transforms to HgI_2-type or cristobalite-like structures at about 3 GPa.

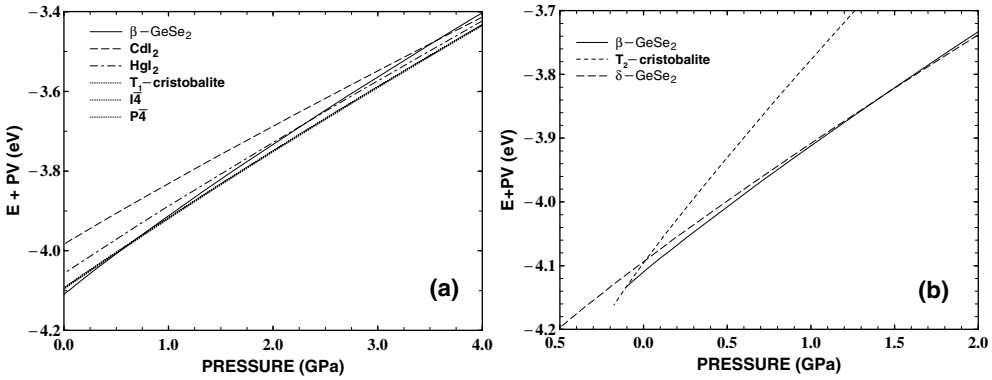

Figure 3. The GGA enthalpy ($E + PV$) versus pressure (P) for the structures studied. (a) The transitions concerning the six synthesized phases of $GeSe_2$. (b) The transitions from β-$GeSe_2$ to the hypothetical structures T_2-cristobalite and δ-$GeSe_2$.

The theoretical prediction of the pressure-induced phase transitions in crystalline $GeSe_2$ can be deduced from our *ab initio* results based on the GGA. We use the GGA instead of the LDA since the GGA has produced results more in line with experiment concerning the energetics of different phases. The enthalpy $E+PV$ versus pressure is plotted in figure 3(a) for the six previously synthesized structures and in figure 3(b) for the two hypothetical structures. In figures 3(a) and (b), the phase of lowest enthalpy at a given pressure is the equilibrium phase at that pressure. Phase equilibria are determined by the Gibbs free energy, but we have neglected the entropy term TS in this analysis and use only the enthalpy. From this, we are able to identify the high-pressure phase transitions involving the studied subset of structures. Figure 3(a) shows such a sequence of phase transitions. The sequence is β-$GeSe_2 \rightarrow T_1$-cristobalite $\rightarrow$ $I\bar{4}$ $\rightarrow$ $P\bar{4} \rightarrow HgI_2 \rightarrow CdI_2$ at pressures of 0.52, 0.67, 0.72, 2.30 and 3.56 GPa, respectively. Comparison with the experiments is difficult since not every transition will occur due to activation barriers that must be overcome, which may be much larger than can be supplied thermally. Experimentally, table 6 suggests the sequence β-$GeSe_2 \rightarrow I\bar{4} \rightarrow$ T_1-cristobalite and/or $\rightarrow HgI_2 \rightarrow CdI_2 \rightarrow P\bar{4}$. This is in qualitatively in agreement with the predicted GGA sequence except for the $P\bar{4}$ phase.

The transitions from β-$GeSe_2$ to the porous hypothetical structures, T_2-cristobalite and δ-$GeSe_2$, are also predicted to occur in figure 3(b). Two possible transitions, β-$GeSe_2 \rightarrow T_2$-cristobalite and β-$GeSe_2 \rightarrow \delta$-$GeSe_2$, are observed occurring at -0.10 GPa and at 1.43 GPa, respectively. The results indicate that porous δ-$GeSe_2$ is a potential high-pressure phase of $GeSe_2$. From the results of figure 3, we conclude that the hypothetical δ-$GeSe_2$ phase is a potential intermediate phase between T_1-cristobalite and HgI_2 type. The supertetrahedral framework, T_2-cristobalite, is an extended framework polymorph of $GeSe_2$ that forms at small negative pressure. Since negative pressure is difficult to produce, other (e.g. templating) means are necessary to produce it. This is similar to semiconductor clathrates, which are easily made and are well studied, but are thermodynamically stable only at negative pressure [42].

4. Electronic properties

The electronic bandstructures of the eight $GeSe_2$ phases studied are shown in figures 4(a)–(h). The bandstructure calculations are based on the LDA-optimized structures since the LDA produces better results than the GGA when compared with available experimental structures.

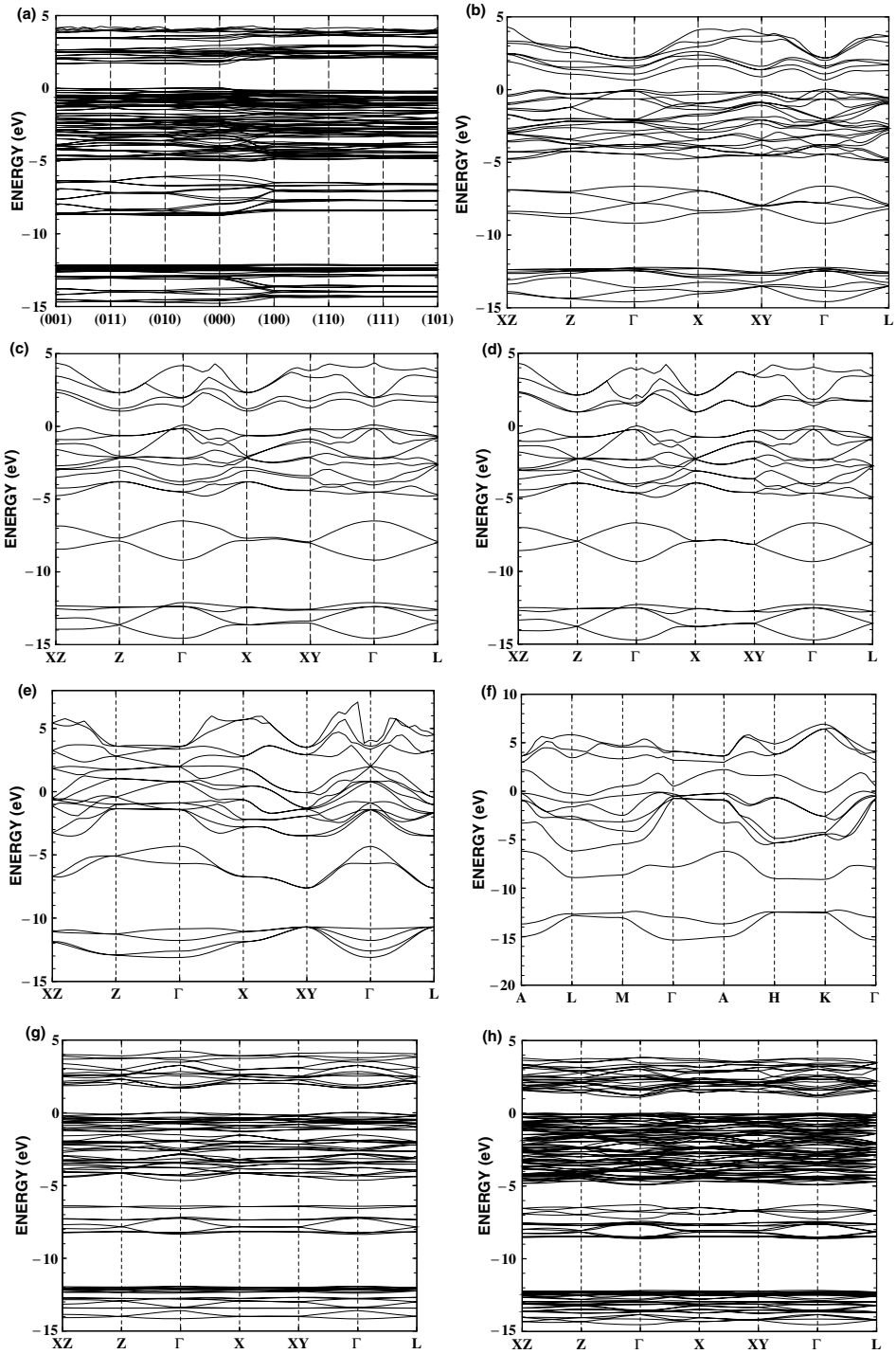

Figure 4. Electronic bandstructures of (a) β-$GeSe_2$, (b) $P\bar{4}$, (c) $I\bar{4}$, (d) T_1-cristobalite, (e) HgI_2-type, (f) CdI_2-type, (g) T_2-cristobalite and (h) δ-$GeSe_2$. The bandstructure calculations are based on the LDA-optimized structures of the phases studied.

The electronic properties from their bandstructures of the six experimental observed phases of $GeSe_2$ can be summarized as follows. β-$GeSe_2$ (figure 4(a)) and $P\bar{4}$-$GeSe_2$ (figure 4(b)) are semiconducting with direct bandgaps at the Γ point of 1.612 and 0.639 eV, respectively. $I\bar{4}$-$GeSe_2$ (figure 4(c)) and T_1-cristobalite (figure 4(d)) are semiconducting with indirect bandgaps of 0.928 and 0.942 eV, respectively. In both $I\bar{4}$ and T_1-cristobalite, the top of the valence band is at Γ and the bottom of the conduction band is at Z or X (within the accuracy of the method, Z and X points are practically degenerate). Both high-pressure phases of the HgI_2-type (figure 4(e)) and the CdI_2-type $GeSe_2$ (figure 4(f)) are found to be metallic.

The fact that CdI_2-type crystalline $GeSe_2$ is a metallic phase is an exciting finding of this work. The semiconductor–metal transition occurring at high pressure in the germanium selenide family has been an attractive and open topic since Prasad *et al* [10] first reported their experimental finding. The important effect of this is that the properties of Ge–Se glass could be permanently changed by applying pressure. It has been found that $GeSe_2$ crystallizes in the CdI_2-type phase at around 7 GPa and it was suggested that this phase is indeed metallic [5, 29]. This phase may account for the semiconductor–metal transition. Our electronic structures of $GeSe_2$ confirm for the first time that the CdI_2-type phase is metallic.

The electronic properties of two hypothetical neutral supertetrahedral porous phases of $GeSe_2$ are also examined. The bandstructure of T_2-cristobalite, figure 4(g), shows that T_2-cristobalite is semiconducting with a direct bandgap at the Γ point of 1.691 eV. δ-$GeSe_2$ (figure 4(h)) is an indirect bandgap semiconductor with an indirect bandgap of 1.04 eV. The bandstructure of δ-$GeSe_2$ shows that the top of the valence band is along Γ–X, while the bottom of the conduction band is at Γ. Further investigation of the charge density distribution showed that there is no significant probability density residing in the pore of either δ or T_2-cristobalite. This means that no electron states are trapped in the pores and therefore we conclude that neither δ nor T_2-cristobalite is an antidot semiconductor. This finding agrees with the result found on neutral supertetrahedral solid $In_4Sn_6S_{18}$ [35].

5. Conclusions

We have studied theoretically the structural and electronic properties of the crystalline $GeSe_2$. The eight phases of $GeSe_2$, six experimentally available and two hypothetical, were investigated under the LDA and the GGA. The correct energetic properties of $GeSe_2$, as well as the qualitative trend of phase transitions, are obtained with the GGA when compared with experiments. β-$GeSe_2$ is the lowest-energy phase among all the structures studied. The two hypothetical porous phases, T_2-cristobalite and δ-$GeSe_2$, are found to be very low-energy phases of the germanium diselenide family. The high-pressure CdI_2-type phase is metallic, which is in line with experimental results that observe a semiconductor to metal transition in $GeSe_2$ glasses speculated to be due to the CdI_2-type phase. Though our results can be used as evidence to support that speculation, we note that (a) the HgI_2 type is also metallic, and (b) we find the CdI_2 type to occur at 3.56 GPa, while HgI_2-type $GeSe_2$ is predicted to occur at 2.30 GPa. Potentially both CdI_2 type and HgI_2 type play a role in the transition.

Acknowledgment

This work is supported by NSF (DMR-99-86706).

References

[1] Nakaoka T, Wang Y, Murase K, Matsuda O and Inoue K 2000 *Phys. Rev.* B **61** 15 569 and references therein
[2] Boolchand P (ed) 2000 *Insulating and Semiconducting Glasses* (Singapore: World Scientific) p 191 and references therein

[3] Fjellåg H, Kongshaug K O and Stølen S 2001 *J. Chem. Soc. Dalton* **7** 1043
[4] Grzechnik A, Stølen S, Bakken E, Grande T and Mezouar M 2000 *J. Solid State Chem.* **150** 121
[5] Grande T, Ishii M, Akaishi M, Aasland S, Fjellåg H and Stølen S 1999 *J. Solid State Chem.* **145** 167
[6] Grzechnik A, Grande T and Stølen S 1998 *J. Solid State Chem.* **141** 248
[7] Popović Z V, Jaksić Z, Raptis Y S and Anastassakis E 1998 *Phys. Rev.* B **57** 3418
[8] Ojima T and Adachi S 1997 *J. Appl. Phys.* **82** 3105
[9] Kandil K M, Kotkata M F, Theye M L, Gheorghiu A, Senemaud C and Dixmier J 1995 *Phys. Rev.* B **51** 17 565
[10] Prasad M V N, Asokan S, Parthasarathy G, Titus S S K and Gopal E S R 1993 *Phys. Chem. Glasses* **34** 199
[11] Durandurdu M and Drabold D A 2002 *Phys. Rev.* B **65** 104208
Cobb M, Drabold D A and Cappelletti R L 1996 *Phys. Rev.* B **54** 162
[12] Cjua-Hua L, Pashinkin A S and Novoselova A V 1962 *Zh. Neorg. Khim.* **7** 2159
[13] Novoselova A V, Zlomanov Yu P, Karbanov S G, Matveyev O V and Gaśkov A M 1972 *Prog. Solid State Chem.* **6/7** 85
[14] Dittmar G and Schäfer H 1975 *Acta Crystallogr.* B **31** 2060
[15] Burgeat J, Le Roux G and Brenac A 1975 *J. Appl. Crystallogr.* **8** 325
[16] Dittmar G and Schäfer H 1976 *Acta Crystallogr.* B **32** 1188
[17] Dittmar G and Schäfer H 1976 *Acta Crystallogr.* B **32** 2726
[18] Godlewski E and laruelle P 1977 *Appl. Crystallogr.* **10** 202
[19] Bletskan D I, Gerasimenko V S and Sichka M Yu 1979 *Kristallographiya* **24** 83
[20] Stølen S, Johnsen H B, Bøe C S, Grande T and Karlsen O B 1999 *J. Phase Equilib.* **20** 17
[21] Kresse G and Furthmüller J 1996 *Comput. Mater. Sci.* **6** 15
[22] Kresse G and Furthmüller J 1996 *Phys. Rev.* B **55** 11 169
Kresse G and Hafner J 1993 *Phys. Rev.* B **47** 558
[23] Vanderbilt D 1990 *Phys. Rev.* B **41** 7892
[24] Monkhorst H J and Pack J D 1976 *Phys. Rev.* B **13** 5189
[25] Ceperly D M and Alder B J 1980 *Phys. Rev. Lett.* **45** 566
[26] Perdew J P and Zunger A 1981 *Phys. Rev.* B **23** 5048
[27] Perdew J P 1991 *Electron Structure of Solids* ed P Ziesche and H Escrig (Berlin: Akademie)
[28] Shimizu Y and Kobayashi T 1983 *Mem. Inst. Sci. Technol. Meiji Univ.* **21** 1
[29] Shimada M and Dachille F 1977 *Inorg. Chem.* **16** 2094
[30] Wells A F (ed) 1984 *Structural Inorganic Chemistry* 5th edn (Oxford: Clarendon) p 194
[31] Bondars B Y, Vitola A A, Miller T N, Ozolinsh G V and Cila Z Y 1977 *Latv. PSR Zinat. Akad. Vestis Khim. Ser.* 632
[32] Boukbir L, Marchand R, Laurent Y, Bacher P and Roult G 1989 *Ann. Chim.* **14** 475
[33] Xun J, Moxom J, Overbury S H and White C W 2002 *Phys. Rev. Lett.* **88** 175502-1
[34] Li H, Eddaoudi M, Laine A, O'Keeffe M and Yaghi O M 1999 *J. Am. Chem. Soc.* **121** 6096
[35] Fuentes-Cabrera M, Wang H, Daniel B and Sankey O F 2002 *Phys. Rev.* B **66** 045109
[36] Stupp S I and Braun P V 1997 *Science* **277** 1242
[37] Ensslin K and Petroff P M 1990 *Phys. Rev.* B **41** 12 307
[38] MacLachlan M J, Coombs N and Ozin G A 1999 *Nature* **397** 681
[39] MacLachlan M J, Petrov S, Bedard R L, Manners I and Ozin G A 1998 *Angew. Chem., Int. Edn Engl.* **37** 2076
[40] O'Keeffe M, Eddaoudi M, Li H L, Reineke T and Yaghi O M 2000 *J. Solid State Chem.* **152** 3 and references therein
[41] Birch F 1952 *J. Geophys. Res.* **57** 227
[42] Ramachandran G K, McMillan R F, Deb S K, Somayazulu S, Gryko J, Dong J and Sankey O F 2000 *J. Phys.: Condens. Matter* **12** 4013